

We are IntechOpen, the world's leading publisher of Open Access books Built by scientists, for scientists

6,900

Open access books available

186,000

International authors and editors

200M

Downloads

Our authors are among the

154

Countries delivered to

TOP 1%

most cited scientists

12.2%

Contributors from top 500 universities



WEB OF SCIENCE™

Selection of our books indexed in the Book Citation Index
in Web of Science™ Core Collection (BKCI)

Interested in publishing with us?
Contact book.department@intechopen.com

Numbers displayed above are based on latest data collected.
For more information visit www.intechopen.com



Nickel Foam Electrode with Low Catalyst Loading and High Performance for Alkaline Direct Alcohol Fuel Cells

Qian Xu, Jiajia Zhang and Chunzhen Yang

Abstract

Nickel foam has a unique three-dimensional (3-D) network structure that helps to effectively utilize catalysts and is often used as an electrode support material for alkaline direct alcohol fuel cells. In this chapter, first, the effect of nickel foam thickness on cell performance is explored. The results show that the thickness affects both mass transfer and electron conduction, and there is an optimal thickness. The thinner the nickel foam is, the better the conductivity is. However, the corresponding three-dimensional space becomes narrower, which results in a partial agglomeration of the catalyst and the hindrance of mass transfer. The cell performance of 0.6 mm nickel foam electrode is better than that of 0.3 and 1.0 mm. Secondly, to fully exert the catalytic function of the catalyst even at a lower loading, a mixed acid-etched nickel foam electrode with lower Pd loading (0.35 mg cm^{-2}) is prepared then by a spontaneous deposition method. The maximum power density of the single alkaline direct ethanol fuel cell (ADEFC) can reach 30 mW cm^{-2} , which is twice the performance of the hydrochloric acid treated nickel foam electrode. The performance improvement is attributed to the micro-holes produced by mixed acids etching, which enhances the roughness of the skeleton and improves the catalyst electrochemical active surface area.

Keywords: nickel foam, thickness, mixed acid, porous skeleton, direct alcohol fuel cell

1. Introduction

Due to the increasing energy consumption and the pollution by fossil fuels, the development of green and environmentally friendly renewable energy sources has won extensive supports from the international community. Ethanol is a kind of low toxicity, high-energy-density liquid fuel, which has the advantages of convenient storage, transportation, and portability. Moreover, ethanol has a wide range of sources, which can be produced from biomass such as corn and sugarcane. Alkaline direct ethanol fuel cell (ADEFC) is an electrochemical power generation device that directly uses ethanol and oxygen with oxidation and reduction reactions at the anode and cathode, respectively. It is an ideal portable power source in the future society with green and efficient characteristics [1–3].

The critical part of a fuel cell is the membrane electrode assembly (MEA), which includes a multi-layer structure of an anode diffusion layer, an anode catalyst layer, a polymer electrolyte membrane, a cathode catalyst layer, and a cathode diffusion layer. Among them, the diffusion layer holds the functions of transporting reactants and products, conducting electrons, and supporting the catalyst layer. Therefore, the performance of the diffusion layer is related to the performance of the fuel cell [4, 5].

The commonly used electrode support materials include carbon paper, carbon cloth, metal foam, etc. Carbon paper is made by carbonizing carbon fiber and binder together. Carbon paper has good uniformity. However, it has poor strength and is easy to break. The ribs of the flow channel on the bipolar plate are also easy to crush the carbon paper during the battery stack assembly process. Carbon cloth is woven from carbon fiber yarn, or is woven into cloth from carbon fiber precursors and then carbonized. Carbon cloth has good strength and is not easy to break. However, due to weaving, the surface flatness of carbon cloth is worse than that of carbon paper. Although the performance of carbon paper and carbon cloth is excellent, the production of carbon paper and carbon cloth requires high-temperature graphitization, the process is complicated, and the technical requirements are high, resulting in high prices of carbon paper and carbon cloth and increasing the cost of fuel cells [6, 7].

Metal foam is a porous metal material that forms countless three-dimensional (3-D) spatial network structures in a metal matrix. It is composed of a rigid framework and internal pores, because it has both metal characteristics and some special physical properties of non-metal, such as porous, lightweight, low density, and high specific strength. There are different types of metal foam, including aluminum foam, titanium foam, copper foam, iron foam, and nickel foam [8]. Among them, nickel foam (Ni foam) is often used as an electrode substrate material in electrochemical energy storage devices, such as secondary nickel-hydrogen, nickel-cadmium batteries, and nickel-zinc batteries, which play a role in collecting current and supporting active materials. The production of Ni foam mainly adopts the electrodeposition method, which uses polyurethane foam as the skeleton. After conductive treatment, electrodeposition and heat treatment are carried out to finally obtain Ni foam [9].

In recent years, Ni foam has been widely used in ADEFC as the electrode support material. The excellent physical properties such as three-dimensional structure, high porosity, high conductivity, and resistance in alkaline media, make the researches of Ni foam develop rapidly. Coupled with the low price of Ni foam, it is more conducive to commercialization.

So far, several works have reported on Ni foams used in fuel cell applications. In 2010, Wang et al. deposited palladium catalyst directly on Ni foam by electrodeposition and found that the three-dimensional porous electrode greatly improved the catalytic activity and stability for ethanol oxidation [10]. In 2011, Li et al. used Ni foam integrated electrode prepared by dip-coating method to perform better on ADEFC than conventional carbon paper electrode [11]. In 2019, Sun et al. further improved the cell performance by improving the electrode preparation method, and the power density reached 202 mW cm^{-2} [12]. It can be found that previous work has demonstrated the application potential of porous electrodes.

By literature survey, it is found that the influence of the physical properties (thickness) of the Ni foam on the cell performance is still unknown. However, the thickness determines the size of the entire three-dimensional space, its own conductivity, and the length of the material transmission path. The thinner the Ni foam, the better the conductivity, but the corresponding three-dimensional space becomes narrower, which may cause agglomeration of part of the catalyst and hinder mass transfer.

At the same time, the smooth skeleton surface of pristine Ni foam results in a low specific surface area, such that a high-load catalyst is required to deal with ethanol oxidation, which increases the cost and limits its application as catalyst support [13]. Hence, efforts to enhance the roughness of the skeleton surface and reduce the catalyst loading have been intensively made. Since an inert layer (oxide layer or hydroxide layer) is easily formed on the surface of Ni foam, it is usually necessary to clean the Ni foam with acid to remove the inert layer before use. As a conventional treatment solution, hydrochloric acid (HCl) is widely used in the literature of Ni foam [6]. However, the HCl treatment can only be used to remove the oxide layer on the surface of the Ni foam without changing the surface roughness of the skeleton.

As early as 1959, W.J. Tegart in his book first proposed a mixed acid solution, glacial acetic acid (CH_3COOH) + nitric acid (HNO_3) + sulfuric acid (H_2SO_4) + phosphoric acid (H_3PO_4), to remove the inert layer on the surface of pure nickel electrode [14]. In 2012, Grdeń et al. first applied this mixed acid solution for the surface etching of Ni foam and found that this etching method can increase the electrochemically active and specific surface areas of Ni foams [15]. In 2019, Zhang et al. used mixed acid-etched Ni foam to the electrocatalytic oxidation of ethanol and obtained better performance [16].

Therefore, in order to explore the influence of the thickness of the Ni foam on cell performance and to fully exert the catalytic function of the catalyst even at a lower loading, in this chapter, firstly, the impact of Ni foam electrodes of different thicknesses on cell performance is discussed. Secondly, a mixed acid-etched nickel foam electrode is explored via the electrode characterization, electrochemical characterization to cell performance test, and the electrode with low palladium loading and high performance is achieved. This work shows the potential for an in-depth exploration of metal foam electrodes.

2. Effect of nickel foam thickness on the performance of an alkaline direct ethanol fuel cell

2.1 Experimental

In this experiment, Nafion 212 membrane is used as an electrolyte membrane, which conducts K^+ for internal ion conduction. The cell principle is shown in **Figure 1**.

2.1.1 Materials and electrode preparation

Three different thicknesses (0.3 mm, 0.6 mm, and 1.0 mm) of Ni foam (110 ppi, Tianyu Heze, China) were cut into 2.0 cm \times 2.0 cm as electrode support materials. Before utilization, the Ni foam needs to be pretreated. First, immerse it in acetone for 20 min. Then, soak it in 1.0 M HCl for 10 min to remove the surface oxide, and finally, rinse it thoroughly with deionized water.

On the anode side, 20 wt.% Pd/C catalyst (Shanxi rock®, China) and 5 wt.% PTFE solution (Hesen®, China) were mixed in isopropanol for preparing the catalyst ink. After stirring the catalyst ink in the ultrasonic bath for 10 min, anode Ni foam electrodes of different thicknesses were prepared by the dip-coating method [11]. The Ni foam is firstly weighed with a scale, then directly immersed in the catalyst ink for 3 min, and finally dried with infrared light for 3 min, and then weighed again. The dipping-drying process was repeated till the 1.0 mg cm^{-2} Pd loading was on the Ni foam to form an electrode.

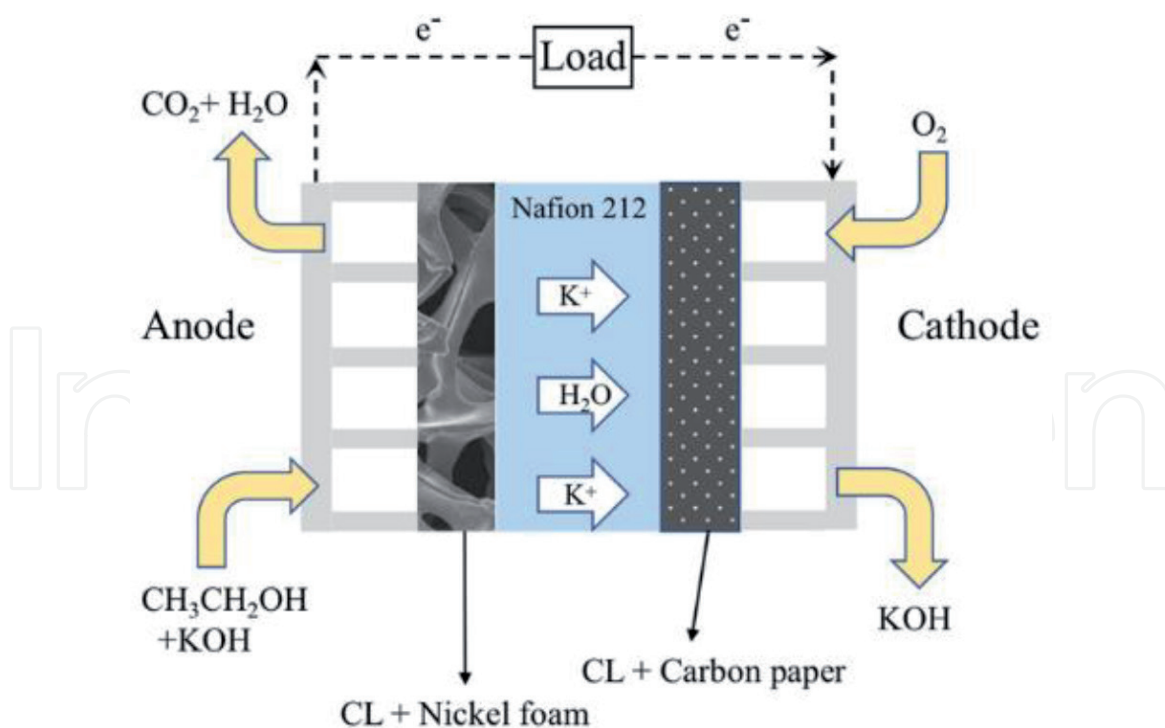


Figure 1.
Schematic diagram of an alkaline direct ethanol fuel cell using Nafion 212 membrane.

On the cathode, a commercial carbon paper electrode (Pt/C nanoparticles with a metallic loading of 2.0 mg cm^{-2} , purchased from Hesen®, China) was applied [17].

2.1.2 Electrode characterization

The X-ray diffraction (XRD) measurement was performed in the D8 ADVANCE diffractometer device (Bruker, Germany), and the Cu $K\alpha$ source was operated at 40 kV and 40 mA. The data is collected in the 2θ range of $20\text{--}90^\circ$ at 5° min^{-1} .

The surface morphology and electrode structure of Ni foam were characterized by a scanning electron microscope (SEM, Hitachi S-3400, Japan).

Cyclic voltammetry (CV) experiments were carried out using a three-electrode cell [18] in an electrochemical workstation (CHI 660E, China) to study the Electrochemical Specific Surface Area (ECSA) of the anode catalyst. Nickel foam electrode, graphite rod, and saturated calomel electrode (SCE) are used as working electrode, a counter electrode, and reference electrode, respectively. At room temperature, the CV curves were tested with a scan rate of 50 mV s^{-1} in 1 M KOH solution saturated with N_2 . The active area of the working electrode is 1.0 cm^2 , and the loaded Pd amount is 1.4 mg.

CHI 660E is used to measure the electrochemical impedance spectroscopy of the ADEFC at 0.4 V [19]. The working temperature of the fuel cell is well controlled at 60°C .

2.1.3 Evaluation of cell performance

The cell performance was evaluated in the MEA composed of a self-made Ni foam anode, commercial carbon paper cathode, and Nafion 212 membrane. Nafion 212 membrane was immersed in 3 M KOH solution for 24 h to enhance the conductivity of K^+ ions and then washed with deionized water before using [20].

The Nafion 212 membrane was sandwiched between the anode and cathode, and a $2.0 \text{ cm} \times 2.0 \text{ cm}$ MEA was assembled without hot pressing. The anode and cathode flow field plates with serpentine flow channels.

During the performance test, the anode was fed with 3 M ethanol and 3 M KOH solution by a peristaltic pump with a flow rate of 1.0 ml min^{-1} , and the cathode was provided dry oxygen with the flow rate of 100 ml min^{-1} .

The cell temperature was controlled at 60°C by a heating rod. The Arbin BT-I fuel cell test system was used to test the performance of a single cell, and the discharge curve was obtained by controlling the current with regular increment.

2.2 Results and discussion

The structural information for clean Ni foam and the Pd/C-Ni foam electrodes were obtained by XRD, as shown in **Figure 2**. In **Figure 2a**, the diffraction pattern

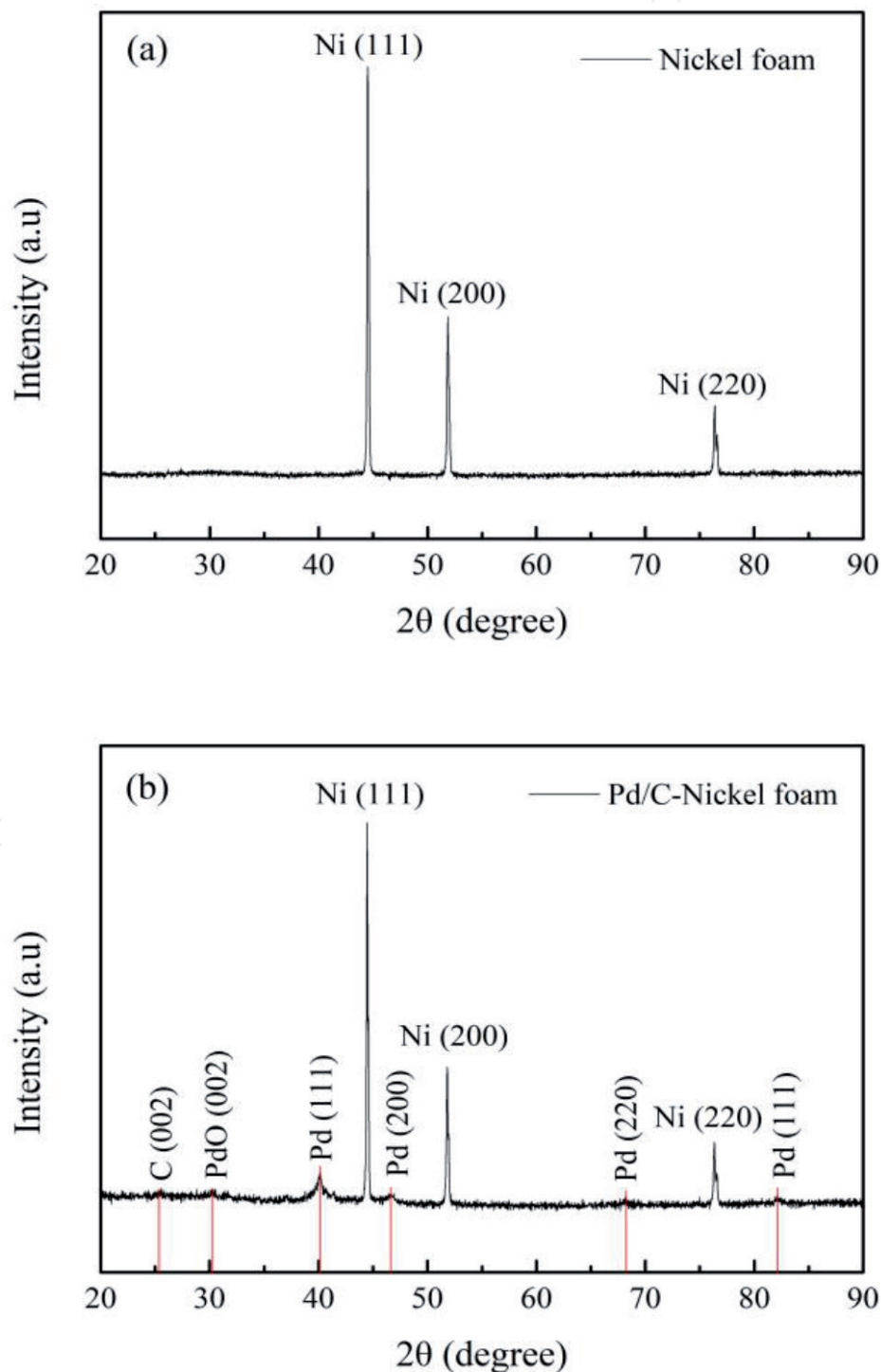


Figure 2.
XRD pattern of (a) the clean Ni foam and (b) the Pd/C-Ni foam electrode.

of a clean Ni foam has three peaks at the 2θ values of 44.50° , 51.85° , and 76.39° , relating with the (111), (200), and (220) planes of the Ni face-centered cubic structure (FCC). It shows that the surface of pretreated Ni foam is clean without impurities.

In **Figure 2b**, the Pd/C-Ni foam electrode exhibits four more peaks at the 2θ of 40.13° , 46.61° , 68.16° , and 82.09° , respectively, corresponding to the (111), (200), and (220) planes of Pd FCC structure. The XRD result indicates that the Pd catalyst is deposited on the Ni foam skeleton. It should be also mentioned that the carbon (002) peak at 25.56° is relatively weak, may be caused by the Pd/C catalyst is mainly distributed inside the three-dimensional structure of Ni foam, while XRD tests the surface of the foam, such that the peak obtained is not notable.

Figure 3a and **b** are the SEM images of clean Ni foam (0.6 mm) after pretreatment. It was found that the original Ni foam skeleton was even, and the porous network structure was regular.

From **Figure 3c**, the catalysts supported on the surface of Ni foam electrode with 0.3 mm thickness are massive and agglomerate severely, so that the catalyst particles wrapped inside do not participate in the catalytic reaction, the ECSA is reduced, and the chemical reaction kinetics weakens. The corresponding cross-sectional view, **Figure 3d** showed the accumulation of the catalyst more clearly and fails to show the advantages of the three-dimensional structure of Ni foam.

It can be seen from **Figure 3e** that the catalyst on the surface of 0.6 mm Ni foam electrode made full use of the supported noble metal catalyst and was evenly supported on the Ni foam skeleton. The even distribution of catalysts on Ni foam skeleton can also speed up the electron transfer. The electrons released by the ethanol oxidation reaction on the outer surface of the Pd catalyst can be fast transferred to the flow field plate through the Ni foam, reducing the electron transfer resistance. At the same time, it can be evidently seen from **Figure 3f** that catalyst loading density was moderate, the pores were more than the 0.3 mm Ni foam, and the mass transfer resistance was smaller.

Similar to that of the 0.6 mm electrode, **Figure 3g** and **h** show the images of the catalyst supported on the 1.0 mm Ni foam electrode. It is regarded that when the thickness of Ni foam exceeds 0.6 mm, the Pd catalyst with 1.0 mg cm^{-2} loading will not have much agglomeration and the catalyst can be distributed evenly on the Ni foam skeleton. However, when the thickness of the Ni foam expands, the path length of the electron transfer will also be larger, which increases the transfer resistance [21].

Figure 4 shows the cell performance of electrodes made of Ni foam with three different thicknesses. When different thicknesses of Ni foam were used, PTFE gaskets of corresponding thickness were used for sealing. As shown in **Figure 4** and **Table 1**, the maximum power densities for 0.3 mm, 0.6 mm, and 1.0 mm Ni foam electrodes were 23.2 , 56.3 , and 32.7 mW cm^{-2} , respectively. The 0.6 mm foam electrode held the highest power density, as 2.4 times higher than that of 0.3 mm and 1.8 times as that of 1.0 mm Ni foam. At the discharging voltage of 0.1 V, the corresponding maximum current densities were 178, 400, and 182 mA cm^{-2} , respectively.

In the low current density region ($<50 \text{ mA cm}^{-2}$), as dominated by the activation polarization and was related to the active sites of catalyst, the cell voltage for 0.3 mm Ni foam electrode dropped sharply from open-circuit voltage (OCV) to 0.34 V. For the 0.6 mm and 1.0 mm thickness electrodes, the trend of voltage drop was quite similar and kept at 0.48 V and 0.46 V, respectively. From **Figure 3c** and **d**, the reason can be found, since 0.3 mm thickness is too thin to support the Pd loading of 1.0 mg cm^{-2} , thus causing catalyst agglomeration and large activation

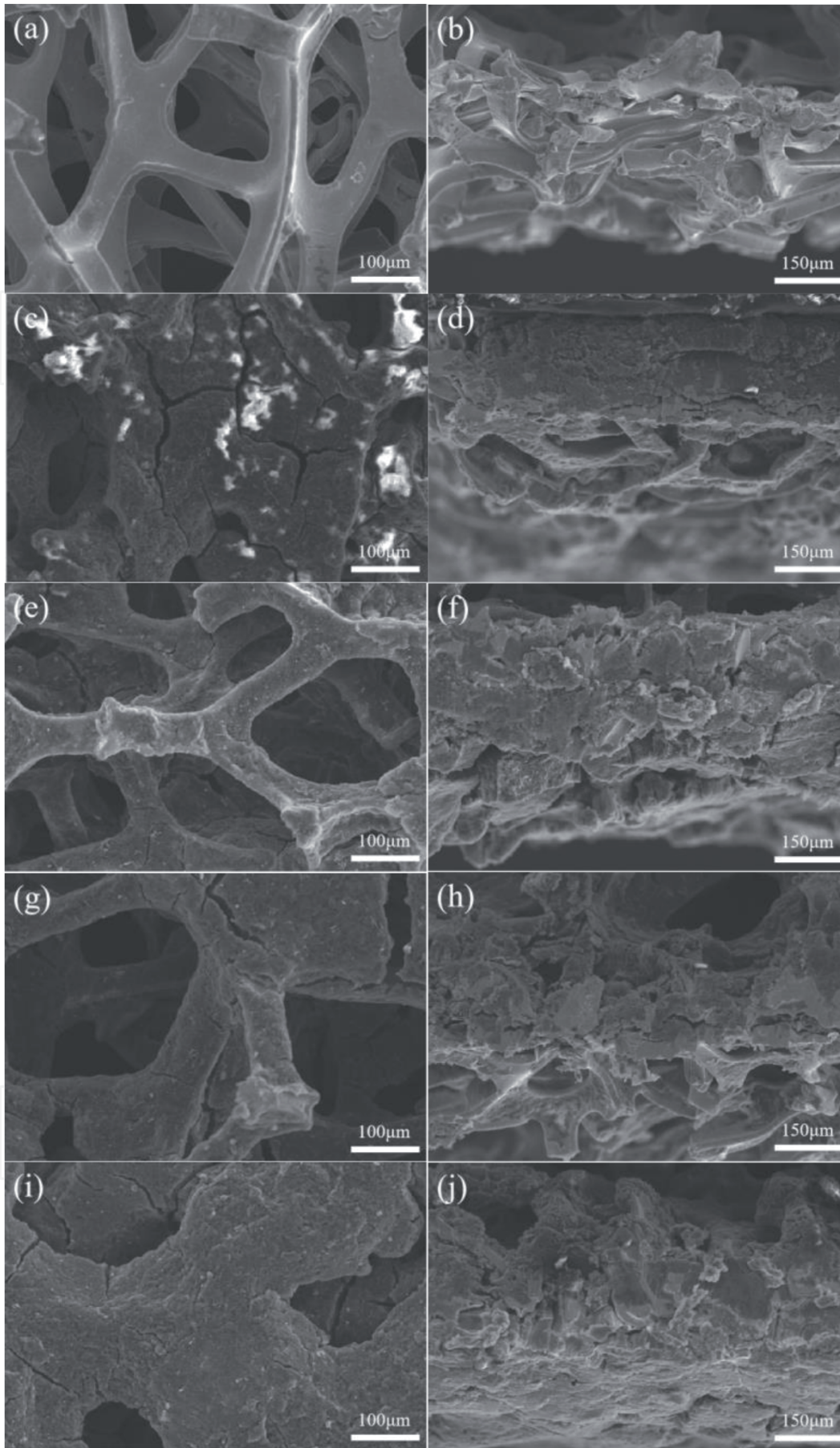


Figure 3. SEM images show the top view of Ni foam electrode with different thickness and different Pd loading. (a) 0.6 mm clean NF, (c) 0.3 mm NF with 1.0 mg cm^{-2} Pd loading, (e) 0.6 mm NF with 1.0 mg cm^{-2} Pd loading, (g) 1.0 mm NF with 1.0 mg cm^{-2} Pd loading and (i) 0.6 mm NF with 2.0 mg cm^{-2} Pd loading. While SEM images (b), (d), (f), (h) and (j) show the cross-sectional morphology of corresponding Ni foam electrode.

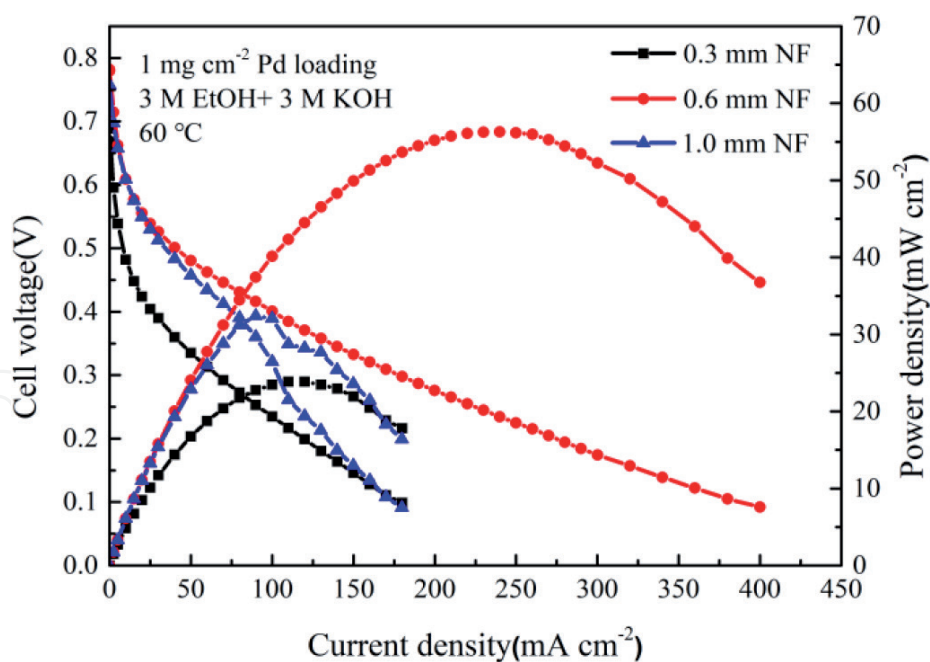


Figure 4.
Cell performance comparison of ADEFC with different thickness of Ni foam electrodes.

Nickel foam thickness (mm)	OCV	50 (mA cm ⁻²)	100 (mA cm ⁻²)	150 (mA cm ⁻²)
0.3	0.67 V	0.34 V	0.24 V	0.15 V
0.6	0.78 V	0.48 V	0.40 V	0.33 V
1.0	0.76 V	0.46 V	0.32 V	0.16 V

Table 1.
Corresponding to the voltage values of several current density points in the above polarization curve.

polarization loss associated with low current densities. However, the electrode of 0.6 mm Ni foam still has enough permeability, which is conducive to the migration of reactant species.

Similarly, in the medium current density range (50–100 mA cm⁻²) controlled by ohmic loss and was related to the resistance of each part of MEA, the voltage of 1.0 mm Ni foam dropped faster than that of the electrode with 0.6 mm Ni foam, which was from 0.48 V to 0.40 V and from 0.46 V to 0.32 V, respectively.

For the high current density region (>150 mA cm⁻²), as controlled by concentration polarization and was mainly related to the mass transfer, only the voltage of 0.6 mm Ni foam electrode could still remain at 0.33 V, implying excellent mass transfer property. This is due to the larger the Ni foam thickness, the longer the electron conduction and mass transfer path, resulting in inferior performance.

In a word, there is an optimal choice between the thickness of the Ni foam electrode and the amount of catalyst loaded, and the thickness should be optimized by considering the trade-off between the electron conduction and mass transfer resistance.

In order to clarify the polarization performances of Ni foam electrodes with different thicknesses, EIS tests were taken as shown in **Figure 5**. The intersection between the high-frequency region and the X-axis represents the ohmic resistance (R1), which is the sum of the electrodes, membrane, and contact resistances. It is mainly dominated by the internal resistance of the membrane [22]. At 0.4 V, the R1 of the 0.3 mm, 0.6 mm and 1.0 mm Ni foam electrodes were 0.414 Ω cm²,

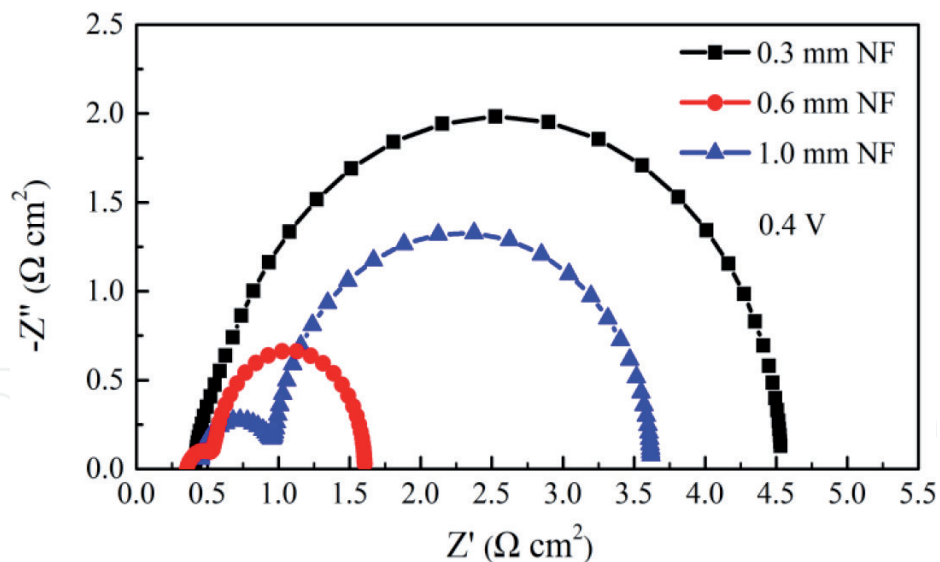


Figure 5.
 EIS comparison of ADEFC with different thickness of Ni foam electrodes at 0.4 V.

0.352 $\Omega \text{ cm}^2$ and 0.445 $\Omega \text{ cm}^2$, respectively. The R1 of the 0.6 mm Ni foam electrode was slightly smaller, as the catalyst distribution on the Ni foam was the most uniform, and the contact between the membrane and the electrode was closer so that the contact resistance was smaller (see **Table 2**).

The value of the intersections of the high and low frequencies on the X-axis can be attributed to the total resistance of charge transfer (cathode and anode), which is also called the electrode reaction resistance (R2). As the exact same commercial cathode electrode is used for each test, the difference in R2 can reflect the difference in anode resistance [23]. The R2 values of the three different thickness Ni foam electrodes were 4.121 $\Omega \text{ cm}^2$, 1.227 $\Omega \text{ cm}^2$ and 3.177 $\Omega \text{ cm}^2$, respectively. It can be found that the better the cell performance, the smaller the electrode reaction resistance. This can be explained as follows: the three-dimensional space of the 0.3 mm Ni foam electrode is narrow, and the catalyst agglomeration is serious, which reduces the catalyst utilization, weakens the EOR kinetics, so that cause the increase of R2. For the 0.6 mm Ni foam electrode, the catalyst is uniformly loaded on the skeleton and almost fully utilized, which contributes to the rapid oxidation of ethanol and reduces the R2. Meanwhile, the 1.0 mm Ni foam electrode has a longer path for electron transfer, which increases the charge transfer resistance, so that a larger R2.

The cyclic voltammetry was used to study the catalytic activity of Ni foam electrodes with different thicknesses in the alkaline medium under the same Pd loading. For each CV curve in **Figure 6**, there was a hydrogen desorption peak at about 0.5 V in the forward potential scan, followed by an OH adsorption peak and an oxidation peak on Pd. In the backward direction scan, there was a reduction peak around 0.6 V, which relates to the reduction of PdO. The reduction current peak is

Nickel foam thickness (mm)	R1 ($\Omega \text{ cm}^2$)	R2 ($\Omega \text{ cm}^2$)
0.3	0.414	4.121
0.6	0.352	1.254
1.0	0.445	3.177

Table 2.
 EIS data of ADEFC with different thickness of Ni foam electrodes at 0.4 V.

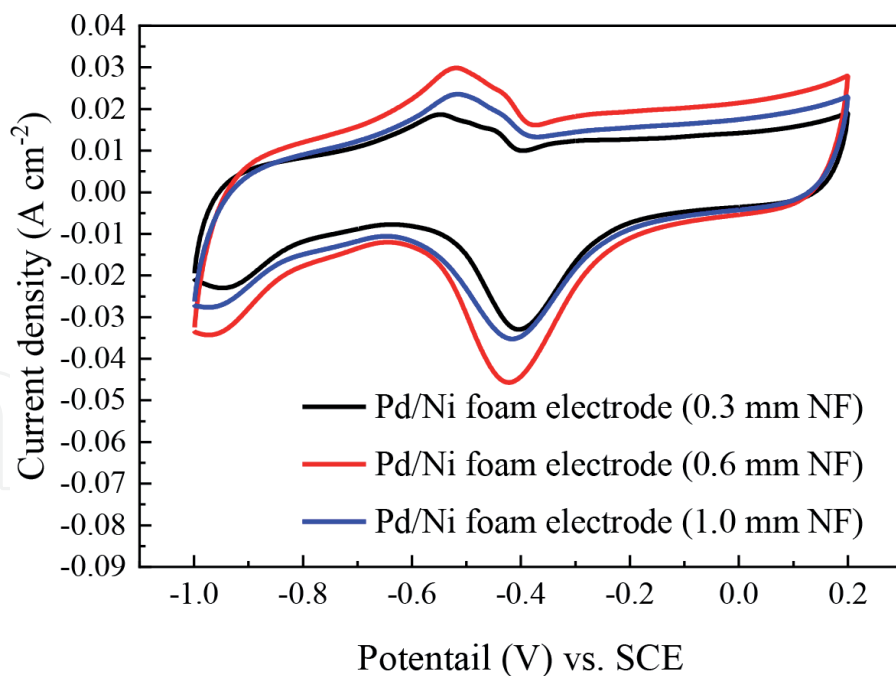


Figure 6. CV curves of the different thickness of Ni foam electrodes in 1 M KOH at a scan rate of 50 mV s^{-1} .

proportional to the amount of OH adsorbed on the Pd surface, such that this can be applied to calculate the ECSA. The larger the ECSA, the more active sites the catalyst holds [24]. The calculation formula of ECSA (Eq. (1)) is as follows:

$$\text{ECSA} = \frac{Q}{qm} \quad (1)$$

where, Q is the coulombic charge obtained by integrating the PdO reduction peak area (μC), m is the Pd loading on the electrode (mg), and q is the charge value of the reduction of PdO of $405 \mu\text{C cm}^2$. The ECSA values of 0.3 mm, 0.6 mm, and 1.0 mm Ni foam electrodes were $11 \text{ m}^2 \text{ g}^{-1}$, $17 \text{ m}^2 \text{ g}^{-1}$ and $15 \text{ m}^2 \text{ g}^{-1}$, respectively, showing that the 0.6 mm Ni foam electrode has the highest ECSA, which can utilize the catalyst better to boost a higher cell performance.

3. A mixed acid-etched nickel foam electrode with ultra-low Pd loading for superior performance of an alkaline direct ethanol fuel cell

3.1 Experimental

3.1.1 Ni foam pretreatment

Firstly, the Ni foam (0.6 mm, 110 ppi, purchased from Heze Tianyu Technology Development Co., Ltd., China) is immersed in acetone and sonicated for 20 min. Next, soak the Ni foam in 5 M HCl for 10 min. Finally, the Ni foam was cleaned with plenty of deionized water.

For comparison, another piece of Ni foam was soaked in anhydrous mixed acids solution (50 g of 99.5 wt.% CH_3COOH + 45 g of 66.5 wt.% HNO_3 + 12 g of 85 wt.% H_3PO_4 + 10 g of 96.5 wt.% H_2SO_4) for 15 s, and the rest of the steps were the same.

3.1.2 Electrochemical characterization

To explore the effect of different acid treatments to remove the Ni foam inert layer, cyclic voltammetry (CV) test was performed in a three-compartment electrochemical cell by an electrochemical workstation (CHI 604E, Shanghai Chenhua Instrument Co., Ltd., China). Cut a piece of 1 cm × 2 cm pretreated Ni foam, use pretreated Ni foam as the working electrode, platinum mesh as the counter electrode, and SCE as the reference electrode. All the potentials applied to refer to an RHE scale. The three electrodes were immersed in 1 M KOH solution, and the electrolyte solution was degassed by bubbling N₂ for 30 min.

To characterize the ECSA and EOR activity of the Pd/Ni foam electrode treated with different acids, a CV test was performed in a three-compartment electrochemical cell by the electrochemical workstation CHI 604E. Cut a piece of 1 cm × 2 cm pretreated Ni foam, and 100 μL 15 mM Na₂PdCl₄ solution was added dropwise to its surface, then 100 μL 5 mM NaBH₄ and 2.5 mM NaOH mixed solution was added dropwise. Thus, the Pd catalyst was chemically reduced on the Ni foam surface to form a Ni foam electrode (Pd/Ni foam) [18]. The area of catalyst deposition was only 1 cm × 1 cm, and the other 1 cm × 1 cm was the part of the working electrode used to collect current. When testing ECSA of the catalyst, the test solution was 1 M KOH. When testing the catalyst activity of EOR, the test solution was a mixed solution of 1 M KOH and 1 M ethanol.

3.1.3 Physical characterization

To observe the surface microstructure, a scanning electron microscope (SEM, Hitachi S-3400, Japan) was tested on the pretreated Ni foam and the Pd/Ni foam electrode.

In order to detect the diffraction peak intensity of metallic Ni on the surface of foam, X-ray diffraction (XRD, Bruker, Germany) was tested on the pretreated Ni foam. Data were collected in the 2θ range 20–90 at 5° min⁻¹.

3.1.4 Cell performance test

Two pieces of 2 cm × 2 cm Ni foam treated with different acids were cut and soaked in 1 mL 15 mM Na₂PdCl₄ solution for reaction. To make sure that the Ni foam surface was sufficiently replaced by Pd, the replacement time was set as 12 h. After drying and weighing, the Ni foam anode was prepared, and Pd loading was 0.35 mg cm⁻². The difference in electrode potential between metals was used to directly replace the catalyst from the precursor solution onto the surface of the Ni foam. The method was simple and no binder was needed [25].

A prepared Ni foam anode, a KOH pre-treated Nafion 212 membrane, and a commercial carbon-paper cathode (Pt/C nanoparticles with a metallic loading of 2.0 mg cm⁻², purchased from Hesen, China) were stacked together to form an MEA. The Nafion 212 membrane was immersed in 3 M KOH solution for 12 h to enhance the K⁺ conductivity of the membrane, where K⁺ realized internal loop circulation [26]. The MEA was placed in a cell fixture with a 2 cm × 2 cm serpentine flow channel made of stainless steel 316L, assembled into a single cell. The Arbin instrument (Arbin BT-I, USA) was used for cell performance testing. The anode was fed with a mixed solution of 3 M KOH and 3 M ethanol, and the peristaltic pump controlled the flow rate to 2 mL min⁻¹. The cathode was fed with normal concentration oxygen, and the rotor flowmeter controlled the flow rate to 100 mL min⁻¹. An external heating rod controlled the cell temperature to 60°C.

3.2 Results and discussion

It can be clearly seen from **Figure 7a** that the pristine Ni foam had a three-dimensional network structure with a disorderly arranged metal skeleton and high porosity. By observing **Figure 7b** and **c**, it was intuitively found that the HCl treatment method did not significantly change the Ni foam skeleton surface, and the metallic nickel layer was still smooth. However, there were obvious changes in the mixed acids treated Ni foam skeleton surface of **Figure 7d** and **e**, with many small holes of about 1 μm in diameter on the skeleton surface, which enhanced the roughness of Ni foam. Meanwhile, these micro-holes existed in the three-dimensional structure of the whole skeleton, which expanded the specific surface area of Ni foam.

The reason for the significant surface difference is that the reaction of Ni foam soaking in HCl solution is mild. HCl without strong oxidizing properties does not react strongly with the metallic nickel, so the surface of the skeleton remains smooth. Whereas, in anhydrous mixed acids solution, CH_3COOH and H_3PO_4 are weak acids with the properties of acid, and HNO_3 and H_2SO_4 are strong acids with strong oxidizing and corrosive properties. Therefore, a short-term immersion treatment could cause a violent redox reaction with metallic nickel. Part of the metallic nickel on the skeleton surface was consumed by the reaction, and the gases produced by the reaction (e.g., NO_2 and SO_2) left dense holes in the skeleton. It should be noted that it was precise because of the strong corrosion ability of the mixed acids that the immersion time should be controlled in a very short time. In this experiment, the soaking time was controlled at 15 s, because the Ni foam was completely dissolved when the soaking time exceeded 1 min.

It can be seen from **Figure 8** that both the Ni foam treated with HCl and Ni foam treated mixed acids had three obvious diffraction peaks at 2θ values of 44.6° , 51.9° and 76.4° , corresponding to the standard diffraction peaks of metallic nickel on (111), (200) and (220) crystal planes (JCPDS. No 04-0850), which indicated that different acid treatment methods did not affect the metallic nickel lattice parameters.

However, by checking the intensity of the diffraction peaks of these two Ni foams, it was not difficult to find that the peak intensities of the (111) and (200) crystal planes of the Ni foam treated with HCl were higher than the corresponding peak intensities of the Ni foam treated with the mixed acids (the black dotted line

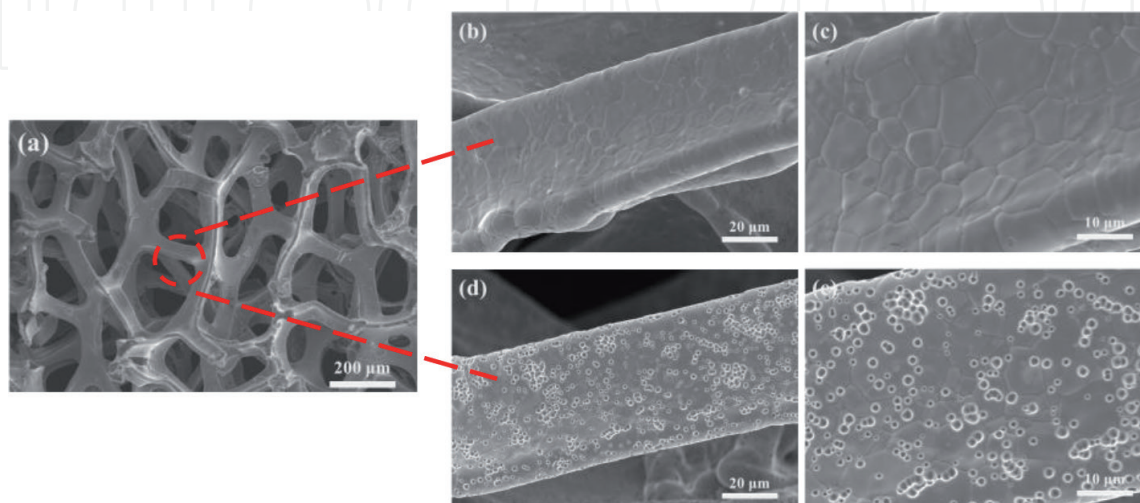


Figure 7. SEM images of (a) pristine Ni foam; (b) Ni foam skeleton treated with HCl; (c) an enlarged view of (b); (d) Ni foam skeleton treated with mixed acids; (e) an enlarged view of (d).

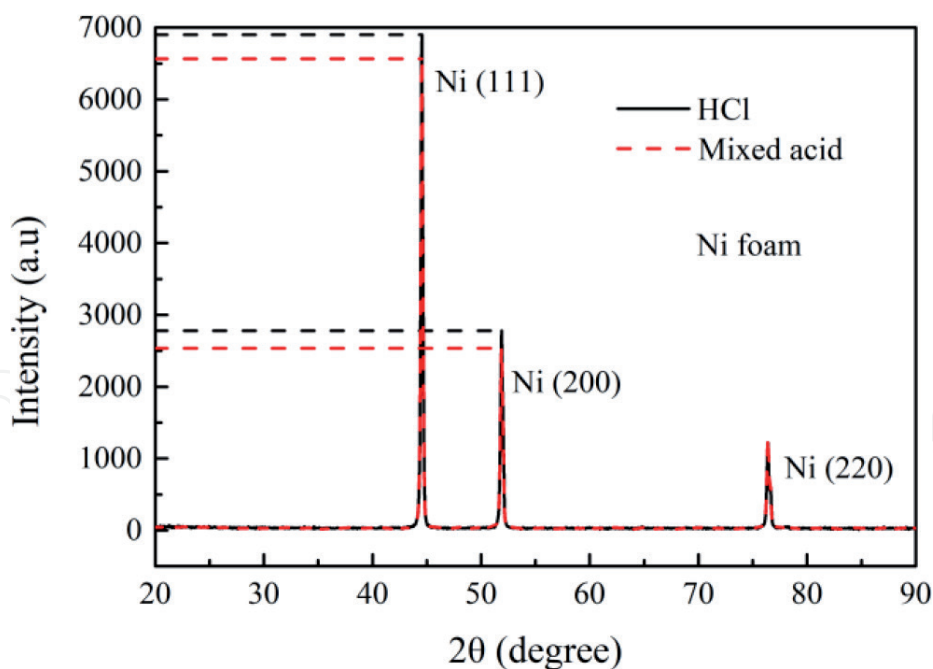


Figure 8.
XRD patterns of Ni foam treated with HCl and Ni foam treated with mixed acids.

above the red dotted line). The reason for this phenomenon is that the mixed acids consume part of metallic nickel during the etching process, resulting in a slight decrease in the X-ray diffraction intensity. It corresponds to the fact that the surface of Ni foam treated with HCl is smooth and neat, while the surface of Ni foam treated with mixed acid is rough, as shown in **Figure 7**.

Figure 9 shows the standard CV curve of the Pd catalyst. In the potential range of 0.1–0.5 V, it corresponded to the hydrogen region. The oxidation peak was H desorption, OH adsorption, while the reduction peak was H adsorption; In the potential range of 1–1.2 V, it corresponded to the oxygen region, where PdO was

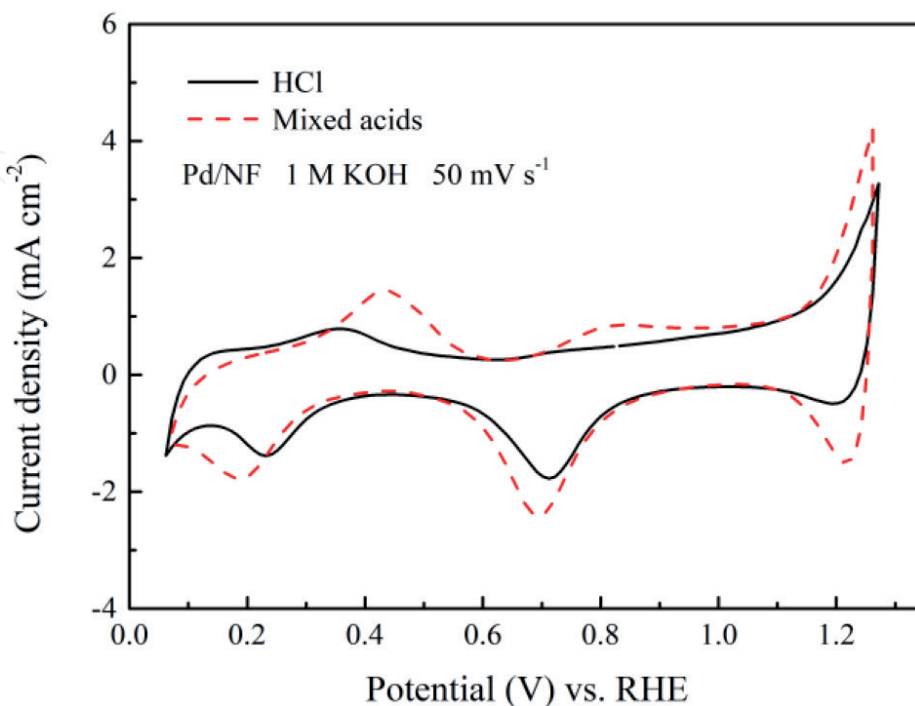


Figure 9.
CV curves of Pd/Ni foam electrode treated with HCl and Pd/Ni foam electrode treated with mixed acids in 1 M KOH solution. Scan rate: 50 mV s⁻¹. Room temperature.

gradually formed, and the corresponding peak at 0.7 V was the reduction peak of PdO. There was an obvious oxidation peak in the potential range of 0.3–0.5 V, and a reduction peak in the potential around 0.1 V, which correspond to the mutual oxidation-reduction between metal Ni and α -Ni(OH)₂, respectively [27]. Also their peaks overlap with the H adsorption/desorption peaks. Generally, the PdO reduction peak was used to compare the electrochemically active area of the Pd catalyst [24].

It also can be seen from **Figure 9** that the Pd/Ni foam electrode treated with mixed acids had a larger ECSA. This result was attributed to a large number of micro-holes formed on the Ni foam skeleton after mixed acids etching. These holes existed greatly increase the specific surface area of Ni foam. When the Pd catalyst was loaded, some of the catalyst particles would be deposited in these holes, which improved the utilization rate of the catalyst. Therefore, the Pd catalyst loaded on the Ni foam treated with mixed acids exposed more active sites and had larger ECSA.

Figure 10 shows the EOR electro-catalytic performance of Pd/Ni foam electrodes treated with different acids. It was found that the maximum current density of the Pd/Ni foam electrode etched by HCl under 0.77 V was only 32 mA cm⁻², while the EOR performance of the Pd/Ni foam electrode etched by mixed acids was much better, as the maximum current density measured at 0.85 V was 56 mA cm⁻². The catalytic performance of EOR has been greatly improved. This was due to the porosity in the nickel skeleton after being etched by the mixed acids, which increased the overall specific surface area. The Pd catalyst was fully utilized, the active sites exposed by the catalyst were more, and the ECSA was higher and the better EOR performance was obtained.

Figure 11 exhibits the preparation process of the Pd/Ni foam electrode. From this figure, it can be seen that the electrode preparation method was simple, and the electrode can be made by immersing only 3 times. **Figures 12** and **13** are the SEM test and cell performance test of the Pd/Ni foam electrode prepared through the preparation process as shown in **Figure 11**.

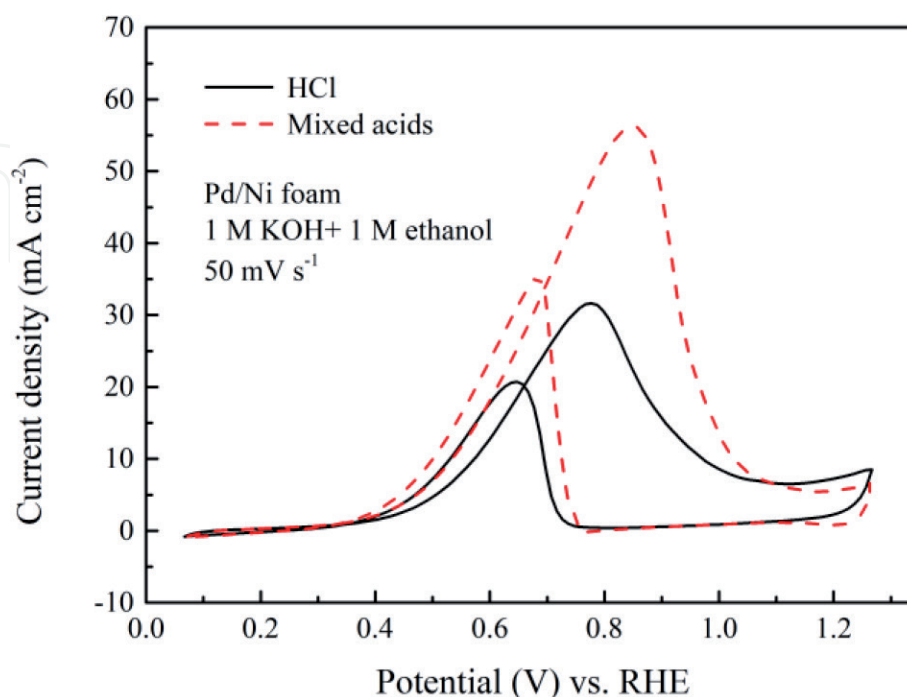


Figure 10. CV curves of Pd/Ni foam electrode treated with HCl and Pd/Ni foam electrode treated with mixed acids in 1 M KOH + 1 M ethanol. Scan rate: 50 mV s⁻¹. Room temperature.

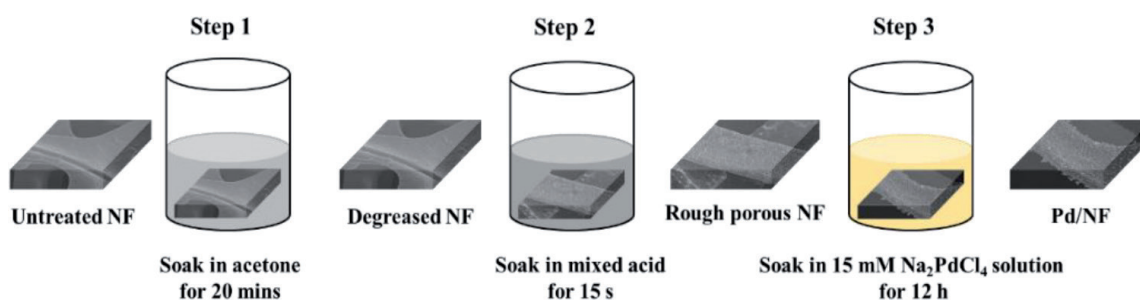


Figure 11.
 Preparation process of Pd/Ni foam electrode.

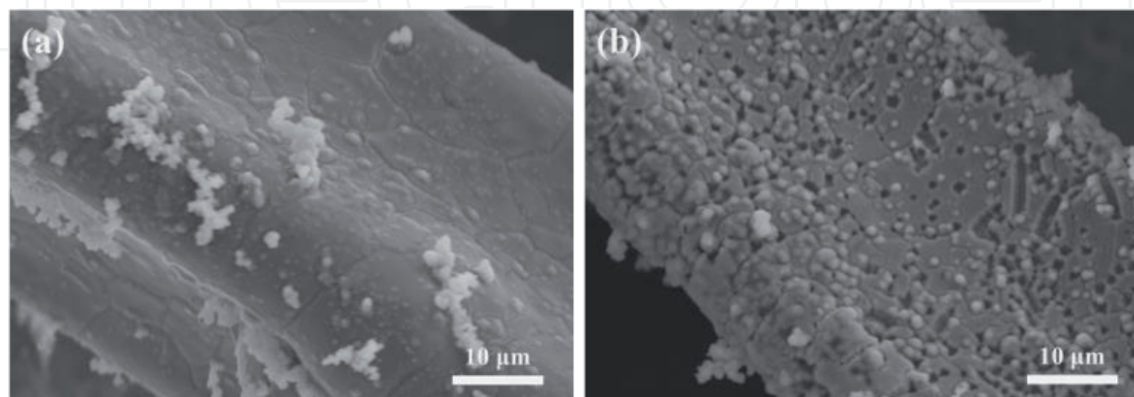


Figure 12.
 SEM images of (a) Pd/Ni foam electrode treated with HCl; (b) Pd/Ni foam electrode treated with mixed acids. The two electrodes were prepared by spontaneous deposition method as shown in Figure 11. Pd loading: 0.35 mg cm^{-2} .

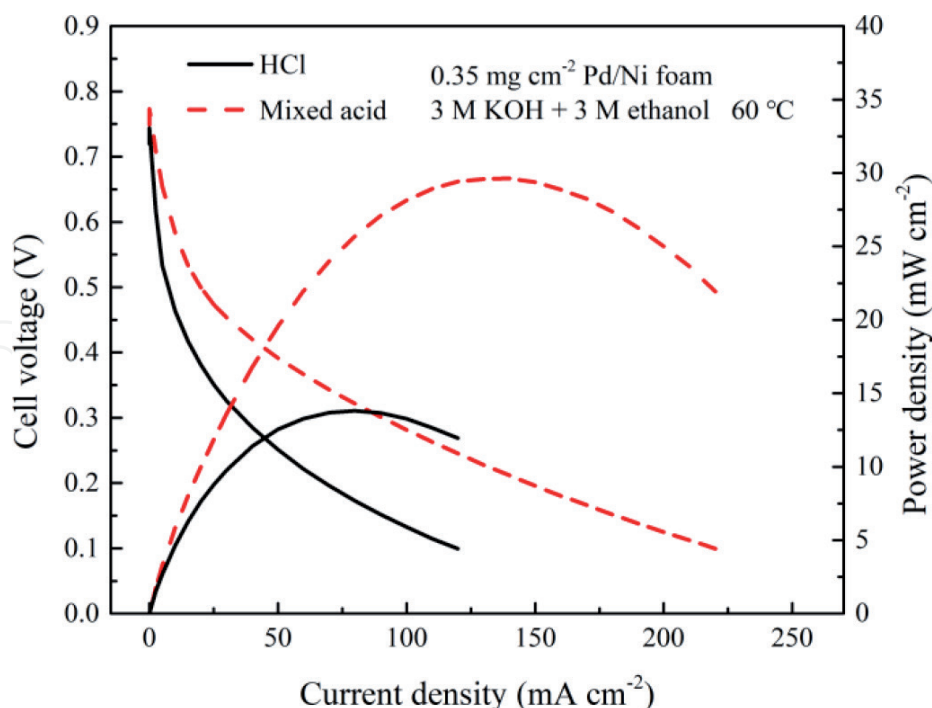


Figure 13.
 Polarization and power density curves of ADEFCs with different acid treated Pd/Ni foam anodes. Pd loading: 0.35 mg cm^{-2} . Test temperature: 60°C. Feeding solution: 3 M KOH and 3 M ethanol aqueous solution.

It can be seen from **Figure 12a** that the Ni foam skeleton was smooth, and the Pd catalyst had uneven load and slight agglomeration on the skeleton surface, which showed that the conventional HCl treatment method reduced the catalyst

Anode	OCV (V)	Maximum current density at 0.1 V (mA cm^{-2})	Peak power density (mW cm^{-2})
Pd/Ni foam treated with HCl	0.719	120	15
Pd/Ni foam treated with mixed acids	0.747	220	30

Table 3.
Important parameter values of cell performance corresponding to **Figure 13**.

utilization. Compared with **Figure 12b**, it was found that the skeleton surface was rough and porous. Most of the Pd particles were uniformly filled in the holes left by the mixed acid etching. These small holes increased the active area of the Pd catalyst.

According to the detailed cell performance information in **Figure 13** and **Table 3**, it can be found that the OCV of the Ni foam electrode treated with HCl was 0.719 V, the corresponding maximum current density at 0.1 V was 120 mA cm^{-2} , and the peak power density was 15 mW cm^{-2} . While the mixed acid-etched Ni foam had excellent cell performance, OCV was 0.747 V, the maximum current density at 0.1 V was 220 mA cm^{-2} , and the peak power density was 30 mW cm^{-2} . Further analysis showed that the cell voltage of the HCl treated electrode dropped quickly from the low current density area. The voltage loss in this area was mainly the activation loss, which was determined by the kinetics of the catalytic oxidation of ethanol and the catalytic reduction of oxygen. Because of the smooth surface of the Ni foam electrode treated by HCl, the catalytic activity was low at low catalyst loading, leading to slow catalytic oxidation of ethanol and a sharp drop in voltage. The Ni foam skeleton etched by mixed acid was rough and porous, which greatly improved the utilization rate of the catalyst and had a high catalyst active area so that even with a small amount of catalyst, it could still exhibit high ethanol oxidation activity and excellent cell performance. This conclusion was also supported by the SEM images in **Figure 12**.

It is worth noting that the prepared electrode applied such a low catalyst loading (0.35 mg cm^{-2} Pd) for single cell test, as to make full use of the advantage that the small holes created by the mixed acids treatment can effectively increase the specific surface area. If the catalyst loading was too high, the catalyst particles would be layered on the Ni foam skeleton. When the skeleton was layered, the catalyst particles filled in the holes would be covered by the upper catalyst layer, which not only failed to reflect the advantages of porosity, but also reduced the utilization of the catalyst inside the holes [28]. It was precise because even with low catalyst loading that higher cell performance was obtained, the superiority of the mixed acid treatment method could be better reflected. This result indicates the potential for in-depth exploration of metal foam electrodes.

4. Conclusions

This work firstly focuses on the effect of different thickness Ni foam anodes on the performance of alkaline direct ethanol fuel cells. The result exhibited that among the 0.3 mm, 0.6 mm, and 1.0 mm thickness Ni foam electrodes, the 0.6 mm thick electrode had the best cell performance, reaching a maximum power density of 56.3 mW cm^{-2} at 60°C , 2.4 times higher than that of 0.3 mm and 1.8 times of that of 1.0 mm. The reason was that the 0.3 mm Ni foam was thin, the catalyst was prone to aggregate on the electrode surface, and was unevenly distributed in the three-dimensional space, leading to the increase of electrochemical reaction resistance

and the decrease of performance. On the other hand, the electron and mass transfer channel of Ni foam with a thickness of 1.0 mm was long, which caused larger polarization. These results have been proven by SEM image, polarization curve test, EIS test, and CV test. It is necessary to optimize the thickness of the Ni foam to more effectively use the catalyst, balance the resistance of electron conduction and mass transfer, and improve the cell performance.

Secondly, the mixed acids etching method is applied to pretreat the Ni foam. It is found that etching can obtain porous skeleton surface, since the strong oxidizing and corrosive nature of the mixed acids can quickly consume the metallic nickel, leaving many micro-holes on the skeleton surface. Using the three-electrode system, it is concluded that the Pd/Ni foam electrode pretreated with mixed acids has a larger ECSA and higher ethanol oxidation activity than HCl. A mixed acid treated Ni foam anode with low Pd loading (0.35 mg cm^{-2}) is prepared by simply soaking three times for ADEFC performance testing. The peak power density reaches 30 mW cm^{-2} , which is double the performance of the HCl treated anode. The performance improvement is attributed to the micro-holes produced by mixed acids etching, which enhance the roughness of the skeleton and improve the ECSA of the catalyst. This work opens a new platform for in-depth exploration on metal foam electrodes.

Acknowledgements

The work described in this chapter was fully supported by Grants from the NSFC, China (No. 51676092), State Key Laboratory of Engine at Tianjin University (No. K2020-14), Six-Talent-Peaks Project in Jiangsu Province (No. 2016-XNY-015), and High-Tech Research Key Laboratory of Zhenjiang City (No. SS2018002).

Conflict of interest

The authors declare no conflict of interest.

Author details

Qian Xu^{1*}, Jiajia Zhang¹ and Chunzhen Yang^{2*}

1 Institute for Energy Research, Jiangsu University, Zhenjiang, China

2 School of Materials Science and Engineering, Sun Yat-Sen University, Guangzhou, China

*Address all correspondence to: xuqian@ujs.edu.cn
and yangchzh6@mail.sysu.edu.cn

IntechOpen

© 2021 The Author(s). Licensee IntechOpen. This chapter is distributed under the terms of the Creative Commons Attribution License (<http://creativecommons.org/licenses/by/3.0>), which permits unrestricted use, distribution, and reproduction in any medium, provided the original work is properly cited. 

References

- [1] Badwal SPS, Giddey S, Kulkarni A, Goel J, Basu S. Direct ethanol fuel cells for transport and stationary applications—A comprehensive review. *Applied Energy*. 2015;**145**:80-103. DOI: 10.1016/j.apenergy.2015.02.002
- [2] Ong BC, Kamarudin SK, Basri S. Direct liquid fuel cells: A review. *International Journal of Hydrogen Energy*. 2017;**42**:10142-10157. DOI: 10.1016/j.ijhydene.2017.01.117
- [3] Fadzillah DM, Kamarudin SK, Zainoodin MA, Masdar MS. Critical challenges in the system development of direct alcohol fuel cells as portable power supplies: An overview. *International Journal of Hydrogen Energy*. 2019;**44**:3031-3054. DOI: 10.1016/j.ijhydene.2018.11.089
- [4] An L, Zhao TS. Transport phenomena in alkaline direct ethanol fuel cells for sustainable energy production. *Journal of Power Sources*. 2017;**341**:199-211. DOI: 10.1016/j.jpowsour.2016.11.117
- [5] Ozden A, Shahgaldi S, Li X, Hamdullahpur F. A review of gas diffusion layers for proton exchange membrane fuel cells—With a focus on characteristics, characterization techniques, materials and designs. *Progress in Energy and Combustion Science*. 2019;**74**:50-102. DOI: 10.1016/j.peccs.2019.05.002
- [6] Tan WC, Saw LH, Thiam HS, Xuan J, Cai Z, Yew MC. Overview of porous media/metal foam application in fuel cells and solar power systems. *Renewable and Sustainable Energy Reviews*. 2018;**96**:181-197. DOI: 10.1016/j.rser.2018.07.032
- [7] Bazylak A, Sinton D, Liu ZS, Djilali N. Effect of compression on liquid water transport and microstructure of PEMFC gas diffusion layers. *Journal of Power Sources*. 2007;**163**:784-792. DOI: 10.1016/j.jpowsour.2006.09.045
- [8] Kuruneru STW, Vafai K, Sauret E, Gu Y. Application of porous metal foam heat exchangers and the implications of particulate fouling for energy-intensive industries. *Chemical Engineering Science*. 2020;**228**:115968. DOI: 10.1016/j.ces.2020.115968
- [9] Paserin V, Marcuson S, Shu J, Wilkinson DS. CVD technique for inco nickel foam production. *Advanced Engineering Materials*. 2004;**6**:454-459. DOI: 10.1002/adem.200405142
- [10] Wang YL, Zhao YQ, Xu CL, Zhao DD, Xu MW, Su ZX, et al. Improved performance of Pd electrocatalyst supported on three-dimensional nickel foam for direct ethanol fuel cells. *Journal of Power Sources*. 2010;**195**:6496-6499. DOI: 10.1016/j.jpowsour.2010.04.025
- [11] Li YS, Zhao TS. A high-performance integrated electrode for anion-exchange membrane direct ethanol fuel cells. *International Journal of Hydrogen Energy*. 2011;**36**:7707-7713. DOI: 10.1016/j.ijhydene.2011.03.090
- [12] Sun X, Li Y, Li MJ. Highly dispersed palladium nanoparticles on carbon-decorated porous nickel electrode: An effective strategy to boost direct ethanol fuel cell up to 202 mW cm⁻². *ACS Sustainable Chemistry & Engineering*. 2019;**7**:11186-11193. DOI: 10.1021/acssuschemeng.9b00355
- [13] Grdeń M, Jerkiewicz G. Influence of surface treatment on the kinetics of the hydrogen evolution reaction on bulk and porous nickel materials. *Electrocatalysis*. 2019;**10**:173-183. DOI: 10.1007/s12678-019-0506-6
- [14] Tegart WJM. The electrolytic and chemical polishing of metals in research and industry. 2nd ed. New York: Pergamon Press; 1959. p. 139. DOI: 10.1002/maco.19600110932

- [15] Grdeń M, Alsabet M, Jerkiewicz G. Surface science and electrochemical analysis of nickel foams. *ACS Applied Materials & Interfaces*. 2012;**4**:3012-3021. DOI: 10.1021/am300380m
- [16] Zhang C, Li CF, Li GR. Pd nanoparticles supported on the etched Ni foams as high-performance electrocatalysts for direct ethanol fuel cells. *Journal of Electrochemistry*. 2019;**25**:571-578. DOI: 10.13208/j.electrochem.181144
- [17] Sun W, Zhang W, Su H, Leung P, Xing L, Xu L, et al. Improving cell performance and alleviating performance degradation by constructing a novel structure of membrane electrode assembly (MEA) of DMFCs. *International Journal of Hydrogen Energy*. 2019;**44**:32231-32239. DOI: 10.1016/j.ijhydene.2019.10.113
- [18] Li Y, He Y. Layer reduction method for fabricating Pd-coated Ni foams as high-performance ethanol electrode for anion-exchange membrane fuel cells. *RSC Advances*. 2014;**4**:16879-16884. DOI: 10.1039/c4ra01399a
- [19] Wu J, Yuan XZ, Wang H, Blanco M, Martin JJ, Zhang J. Diagnostic tools in PEM fuel cell research: Part I electrochemical techniques. *International Journal of Hydrogen Energy*. 2008;**33**:1735-1746. DOI: 10.1016/j.ijhydene.2008.01.013
- [20] Hou H, Wang S, Jin W, Jiang Q, Sun L, Jiang L, et al. KOH modified Nafion112 membrane for high performance alkaline direct ethanol fuel cell. *International Journal of Hydrogen Energy*. 2011;**36**:5104-5109. DOI: 10.1016/j.ijhydene.2010.12.093
- [21] Tseng CJ, Tsai BT, Liu ZS, Cheng TC, Chang WC, Lo SK. A PEM fuel cell with metal foam as flow distributor. *Energy Conversion and Management*. 2012;**62**:14-21. DOI: 10.1016/j.enconman.2012.03.018
- [22] Yang SH, Chen CY, Wang WJ. An impedance study of an operating direct methanol fuel cell. *Journal of Power Sources*. 2010;**195**:2319-2330. DOI: 10.1016/j.jpowsour.2009.10.066
- [23] Guo J, Chen R, Zhu F-C, Sun S-G, Villullas HM. New understandings of ethanol oxidation reaction mechanism on Pd/C and Pd₂Ru/C catalysts in alkaline direct ethanol fuel cells. *Applied Catalysis B: Environmental*. 2018;**224**:602-611. DOI: 10.1016/j.apcatb.2017.10.037
- [24] Ma L, Chu D, Chen R. Comparison of ethanol electro-oxidation on Pt/C and Pd/C catalysts in alkaline media. *International Journal of Hydrogen Energy*. 2012;**37**:11185-11194. DOI: 10.1016/j.ijhydene.2012.04.132
- [25] Niu X, Zhao H, Lan M. Palladium deposits spontaneously grown on nickel foam for electro-catalyzing methanol oxidation: Effect of precursors. *Journal of Power Sources*. 2016;**306**:361-368. DOI: 10.1016/j.jpowsour.2015.12.044
- [26] Zakaria Z, Kamarudin SK, Timmiati SN. Membranes for direct ethanol fuel cells: An overview. *Applied Energy*. 2016;**163**:334-342. DOI: 10.1016/j.apenergy.2015.10.124
- [27] van Drunen J, Kinkead B, Wang MCP, Sourty E, Gates BD, Jerkiewicz G. Comprehensive structural, surface-chemical and electrochemical characterization of nickel-based metallic foams. *ACS Applied Materials & Interfaces*. 2013;**5**:6712-6722. DOI: 10.1021/am401606n
- [28] Zhang J, Zhang W, Xing L, Su H, Xu Q. Experimental investigation on the effect of mixed acids etched nickel foam electrode on performance of an alkaline direct ethanol fuel cell. In: 2020 5th International Conference on Advances in Energy and Environment Research (ICAEEER 2020); 18-20 September 2020; Virtual, Online. Vol. 194. China: EDP Sciences; 2020. p. 02021